Applied Geochemistry 138 (2022) 105234

Contents lists available at ScienceDirect

Applied Geochemistry

journal homepage: www.elsevier.com/locate/apgeochem

Porewater chemistry of Opalinus Clay revisited: Findings from 25 years of data collection at the Mont Terri Rock Laboratory

Paul Wersin [a,*], Martin Mazurek [a], Thomas Gimmi [a,b]

[a] Rock-Water Interaction, Institute of Geological Sciences, University of Bern, Baltzerstrasse 1+3, 3012, Bern, Switzerland
[b] Laboratory for Waste Management, Paul Scherrer Institut, 5232, Villigen, Switzerland

ARTICLE INFO

Editorial handling: Dr. Z Zimeng Wang

Keywords:
Clayrock
Porewater chemistry
Database
Opalinus Clay
Mont Terri project

ABSTRACT

The characterisation of porewater chemistry in nanoporous clayrocks is a difficult task. Appropriate extraction methods that have been developed fairly recently and the Mont Terri Rock Laboratory (Switzerland) have played a pioneer role in this regard. During the last 25 years high-quality data from the Opalinus Clay have been acquired. Notably, since the early synthesis of Pearson et al. (2003) a considerable number of newer data from borehole waters and waters extracted from drillcores have been generated. In this study, borehole, squeezing, leaching and cation exchange data were critically evaluated in order to derive a consistent porewater chemistry database across the formation. The results underline that the porewater composition is not constant but exhibits a regular change towards the formation boundaries. This is explained by diffusive exchange between the Na–Cl type porewater and the two bounding freshwater aquifers. Furthermore, the porewater is constrained by cation exchange, carbonate mineral and celestite equilibria. Major solute data obtained from borehole waters and squeezed waters are broadly consistent, although the latter exhibit somewhat more scatter. Overall, the knowledge on porewaters at the Mont Terri Rock Laboratory has been significantly improved. In particular, this regards the spatial profiles of major elements besides Cl, and better constraints on exchanger composition and pH/pCO_2 conditions.

1. Introduction

Argillaceous rock formations (termed clayrocks hereafter) often exhibit very low permeabilities. They may act as natural barriers and thus serve as caprocks for oil and gas reservoirs or as host rocks for radioactive waste repositories. In the context of the latter, it is important to thoroughly characterise the host rock for safety assessment. For example, this regards the porewater chemistry of the clayrock, since it affects the properties of the engineered barrier system (e.g. swelling behaviour of the bentonite barrier) and the transport of radionuclides eventually released upon breaching of the waste canister (Altmann, 2008).

The intimate association of porewater with the nanoporous clayrock and the low permeability inhibit sampling of porewater by conventional water sampling techniques and make the characterisation of porewater chemistry a difficult task (Sacchi et al., 2000). A number of extraction methods exist, but virtually each of them may create disturbances and alter the in-situ porewater chemistry. Methods to characterise porewaters in clayrock have been developed fairly recently – mainly in the light of interest related to radioactive waste disposal. The Mont Terri Project, supported by an international consortium, has played a pioneer role in this regard (Thury and Bossart, 1999; Bossart and Thury, 2008). One of the main goals in this project has been to develop methods to characterise the porewater chemistry in Opalinus Clay (OPA), a Mesozoic clayrock foreseen as host rock for geological disposal of radioactive waste in Switzerland (Nagra, 2002). This includes in-situ experiments in the Mont Terri Rock Laboratory, complemented by laboratory studies and modelling approaches. An important milestone in this context was the synthesis report of Pearson et al. (2003), in which these methods were presented and discussed. During the last 15 years, a number of further studies related to porewater chemistry have been carried out within the Mont Terri Project (e.g. Courdouan et al., 2007; Courdouan Merz 2008; Fernández et al., 2007; Vinsot et al., 2008; Wersin et al., 2009; Pearson et al., 2011; Wersin et al., 2011; Gimmi et al., 2014; Fernández et al., 2014; Vinsot et al., 2014; Bleyen et al., 2017; Mazurek et al., 2017; Waber and Rufer 2017; Rufer et al., 2018). These have generated valuable data on porewater chemistry of the OPA. A coherent evaluation of the ensemble of these data in terms of the in-situ porewater

* Corresponding author.
E-mail address: paul.wersin@geo.unibe.ch (P. Wersin).

https://doi.org/10.1016/j.apgeochem.2022.105234
Received 20 November 2021; Received in revised form 25 January 2022; Accepted 4 February 2022
Available online 9 February 2022

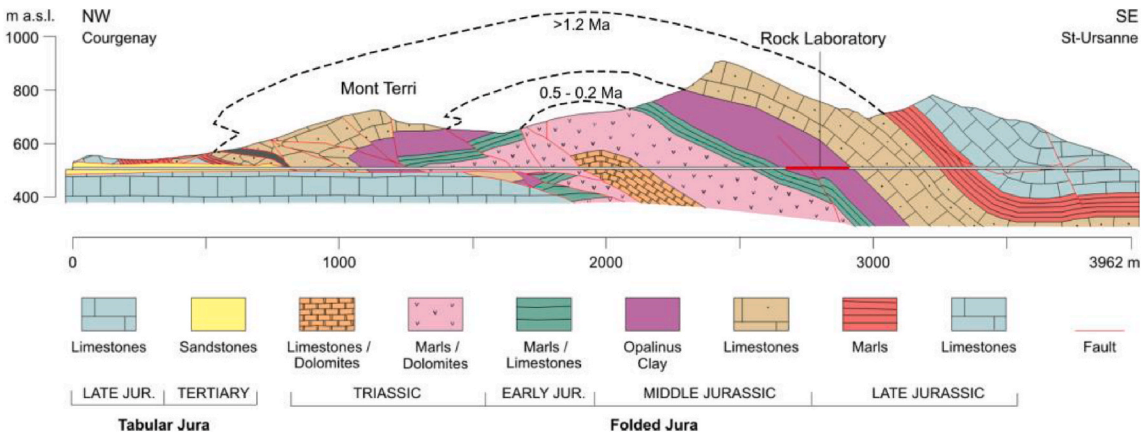

Fig. 1. Geological profile across the Mont Terri anticline. Schematic representation of erosion history (modified from Freivogel and Huggenberger, 2003).

conditions is however lacking to date.

The overall objective of this work was to refine the knowledge on the porewater chemistry of OPA at the Mont Terri site. This was done by critical selection and evaluation of water samples extracted from (i) packed-off boreholes, (ii) squeezed waters from drillcores and (iii) aqueous leachates from drillcores (the latter for refinement of the chloride and bromide profiles). Moreover, data obtained from selected cation exchange experiments were included in the analysis. The data screening aimed at obtaining data with no obvious signs of perturbations (e.g. oxidation by ingress of O_2) on the one hand and to obtain a database representative of the local porewater composition across the entire formation on the other hand. The final goal of the proposed database was to provide a sound basis for modelling of the OPA porewaters, including equilibrium modelling and multicomponent reactive transport modelling.

2. Background information

2.1. Geologic and hydrogeologic setting

The Mont Terri Rock Laboratory is situated in NW Switzerland close to the town of St. Ursanne. It consists of a gallery system connected to the motorway tunnel which transects an asymmetric anticline structure in the Jura fold-and-thrust belt, comprising limestones, marls and clayrocks of Triassic to Jurassic age (Fig. 1). The rocks are strongly tectonised, but the deformation and structural complexity is least developed in the SE part of the anticline (Bossart, 2007). In this area, the rock laboratory is located and transects the OPA in its entire thickness. The strata dip to the SE with an angle between 22° in the south and 55° in the north. The largest structure cross-cutting the laboratory, the so-called Main Fault, is considered to be an internal detachment horizon within the OPA. The maximum overburden above the rock laboratory is about 300 m.

According to the rock parameter database for OPA compiled by

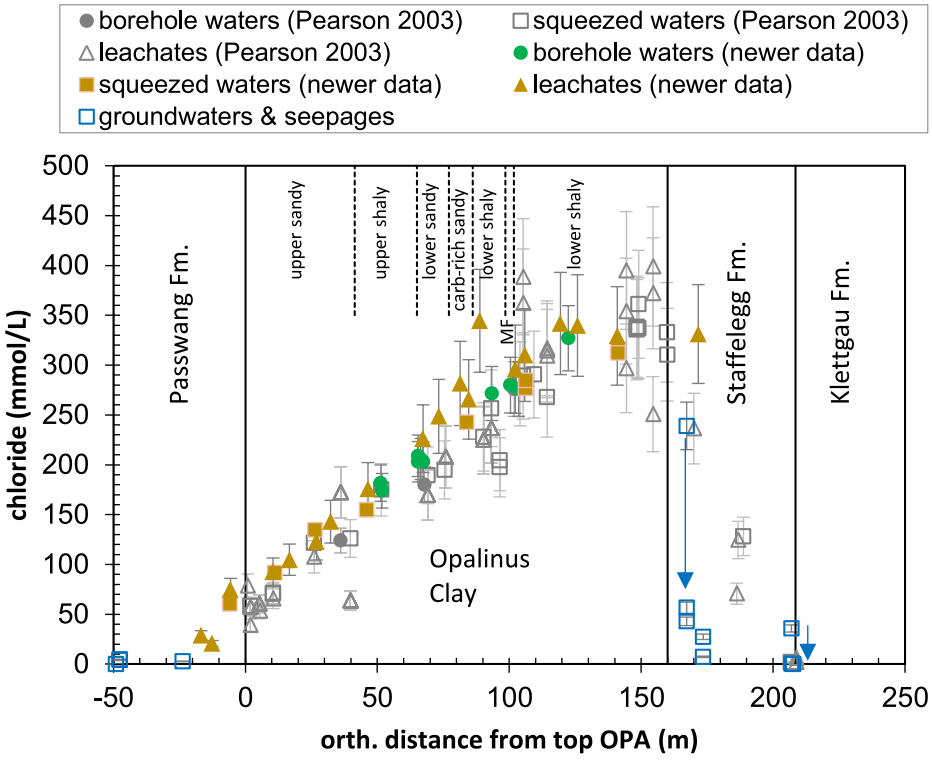

Fig. 2. Chloride concentrations as function of orthogonal distance from the OPA/Passwang Fm. contact. Borehole waters, squeezed waters and leachates from Pearson et al. (2003) (grey symbols). Newer data includes borehole waters, squeezed waters and leachates (green and brown symbols). Samples from bounding aquifers and seepage waters are also shown (blue symbols). Leachates re-calculated considering water-loss porosity and average anion-accessible porosity fraction of 0.54. Errors: 5% (based on analytical error) for newer squeezed waters, 10% (based on analytical error and time-dependent variations) for borehole & seepage waters, "old" squeezed waters and groundwaters, 15% (based on combined analytical error and errors related to water content and anion-accessible porosity fraction) for leachates. Arrows show temporal evolution of a seepage water and groundwater in the Staffelegg Fm. (Gautschi et al., 1993). MF: Main fault. (For interpretation of the references to colour in this figure legend, the reader is referred to the Web version of this article.)

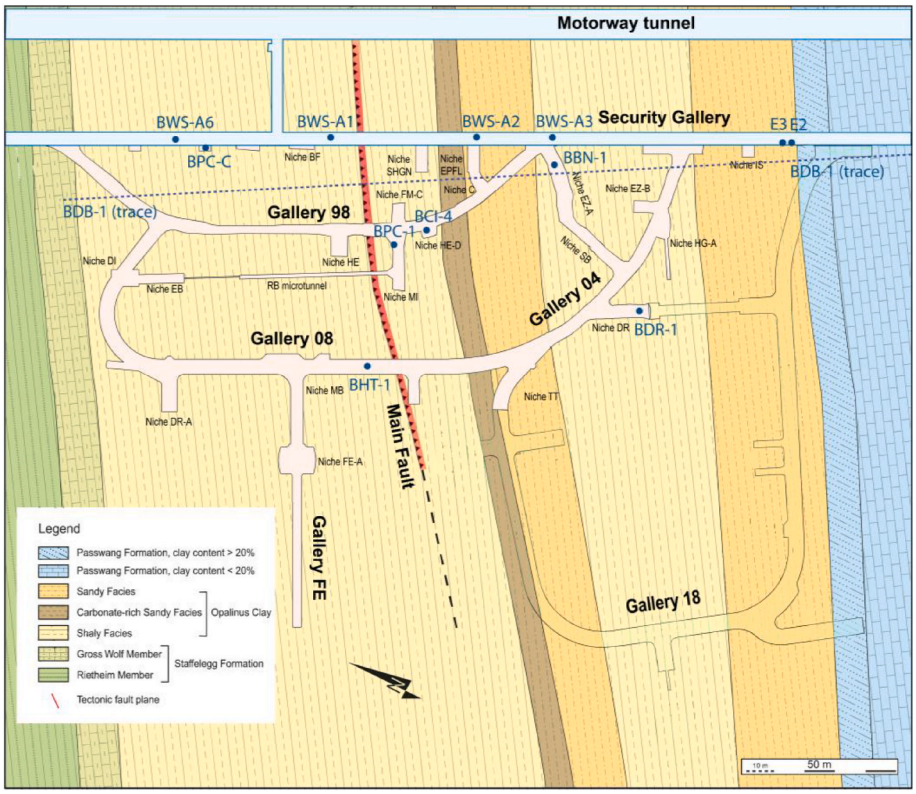

Fig. 3. Location of selected boreholes (borehole mouth) in which porewaters and drillcores were extracted (modified from map provided by D. Jäggi, swisstopo). For BDB-1 borehole (DB-A experiment) a projection parallel to bedding is shown as dashed blue line; the borehole mouth lies outside the displayed area. (For interpretation of the references to colour in this figure legend, the reader is referred to the Web version of this article.)

Mazurek (2017), the main mineral fractions are (in wt% ±1σ): clay minerals (52.9 ± 14.9), quartz (21.4 ± 9.6) calcite (18.2 ± 11.7) and feldspars (3.3 ± 2.2). The clay minerals in the fraction <2 μm include mainly illite, illite/smectite mixed layers and kaolinite, whereas chlorite contents are subordinate. Lithologically, OPA can be subdivided into five subunits, from bottom to top: lower shaly, sandy and carbonate-rich, lower sandy, upper shaly and upper sandy facies (Pearson et al., 2003; Reisdorf et al., 2014). Note that the lower shaly facies is richer in clay minerals than the upper one, and the lower sandy facies has substantially more quartz and less clay minerals than the upper sandy facies. A more accurate nomenclature has been recently elaborated by (Mazurek and Aschwanden, 2020). The proportions of the main minerals vary between the different subunits, but the clay mineralogy does not exhibit notable differences in the relative proportions of the different clay minerals. Furthermore, all subunits contain siderite (2.6 ± 2.3), dolomite/ankerite (0.5 ± 0.5), pyrite (1.2 ± 1.0) and organic carbon (0.7 ± 0.4) (Mazurek, 2017). Diagenetic celestite has been observed at low levels (<0.1 wt%) in different subunits (see section 4.4).

The OPA is underlain by Liassic clayrocks, marls and limestones (Staffelegg Fm.) and overlain by Dogger limestones (Passwang Fm.). These bounding units contain local aquifers which form the current hydrogeological boundaries of the aquitard comprising the OPA, the lowest beds of the Passwang Fm. and the underlying Liassic clayrocks. The overall thickness of the low permeability sequence at the rock laboratory level is about 219 m (Mazurek et al., 2009). The palaeo-hydrogeological evolution is linked to the erosion history and activation of the two bounding aquifers upon exhumation. From geological arguments, Bossart and Wermeille (2003) estimated the exhumation and activation of the upper aquifer in the Dogger limestones to have occurred in the interval 10.5–1.2 Ma (Fig. 1). The Liassic limestone aquifer underlying the OPA, situated in the core of the anticline, was activated later when the OPA had partly been eroded away. Bossart and Wermeille (2003) estimated that this occurred at 0.5–0.2 Ma. Hence, the evolution of freshwater infiltration into both aquifers was controlled by the erosion of the anticline, which resulted in a considerable lag of the activation of the lower aquifer compared to the upper one.

2.2. Distribution of chloride

Fig. 2 shows the spatial distribution of chloride across the OPA. Older data from Pearson et al. (2003) as well as more recent data, as presented in this work, indicate an asymmetric curved trend. Using geologically reasonable boundary conditions, such as the erosional history of the site, Mazurek et al. (2009, 2011) modelled the profile of Cl and other tracers by 1D diffusive exchange with the bounding aquifers. It could be shown that diffusion alone could describe the observed profiles without adding an advective component across the OPA. The asymmetry of the profile was explained by the time lag between the activation of the upper and the lower aquifer. A main uncertainty was found to be the definition of initial conditions.

Chloride data shown in Fig. 2 also includes analyses of aqueous leachates. These yield the Cl inventory in the total porewater, but not directly the concentration in the anion-accessible porosity fraction. The re-calculation is commonly done by assuming a given porosity-fraction accessible to chloride. The concept behind is that anions are repelled from the negatively charged clay surface and thus only "see" a part of the porosity (anion exclusion or geochemical porosity concept, e.g. Pearson 1999). Pearson et al. (2003) considered an anion porosity fraction of 0.54 of the total porosity for the entire OPA profile at Mont Terri based on the analysis of leachates, squeezed waters and borehole waters. There are more advanced concepts for describing the distribution of anions and cations in clayrocks (e.g. Appelo and Wersin, 2007; Tournassat and

Steefel, 2015), but they depend on several generally uncertain parameters, while the simple concept has been shown to be useful for interpreting porewater chemistry data derived from different methods (Pearson et al., 2011; Tournassat et al., 2015). It should be noted that errors on leachate data are generally larger because of the errors related to the re-calculation to the anion-accessibly porosity compared to the data obtained from direct measurements.

3. Data selection

3.1. Strategy

A large number of porewater data have been acquired over the last 25 years at the Mont Terri Rock Laboratory. This primarily includes samples from packed-off boreholes and high-pressure squeezing of drillcores. The extracted porewaters and drillcores may be affected by chemical and microbial perturbations during borehole installation, sampling and experimental procedures (Sacchi et al., 2000). Bearing this in mind, the methodological practices have been successively improved. For example, several boreholes were drilled using inert gases (N_2, Ar) rather than air to reduce ingress of O_2 into the test interval (e.g. Vinsot et al., 2008), and inert equipment materials (e.g. Teflon) were emplaced (e.g. Gimmi et al., 2014).

The strategy of the data selection was two-fold: (i) obtain a representative dataset across the entire OPA formation and (ii) focus on data deemed to be of good quality, that is, acquired with appropriate procedures to limit effects of perturbations, such as oxidation due to air ingress. Thus, in general peer-reviewed data was selected. Moreover, if possible, time series of sampled borehole waters were considered. The origin of all data used in this work is listed in Appendix D (Table D-1).

3.2. Borehole waters & seepage waters/groundwaters

Two types of experimental setups were considered to sample waters from boreholes:

1) Seepage of porewaters via a hydraulic gradient into a packed-off interval of an ascending borehole (seepage borehole waters);
2) Injection of artificial porewater into a descending packed-off borehole which diffusively equilibrates via a filter with the surrounding porewater (diffusively equilibrated borehole waters).

The methodology for acquiring and analysing water samples from boreholes presented here can be found in Pearson et al. (2003) and Wersin et al. (2020).

The location of the boreholes is shown in Fig. 3. Below follows a list of the corresponding experiments.

WS-A experiments: In the experiments WS-A1, WS-A2 and WS-A3, seepage borehole waters were sampled from three ascending boreholes (BWS-A1, BWS-A2 and BWS-A3) since the late 1990^{ies}. The boreholes were drilled with air but the test interval was filled with N_2. The early data up to the year 2000 were critically reviewed by Pearson et al. (2003) who defined "reference water analyses" deemed of reasonably good quality. Regular sampling was further carried out during the period 2003–2006 (Courdouan Merz, 2008). The two datasets were selected for this work and presented in Table A-1 in Appendix A. Analytical errors for major solutes are reported to be 5% but the overall uncertainty may be higher as indicated for example from comparison of analyses obtained by different laboratories (Pearson et al., 2003). For minor solutes, the analytical error is 10–15%.

PC-C experiment: In this experiment, an ascending borehole BPC-C1 was drilled with N_2 in 2004 and then the test interval was filled with Ar which was continuously circulated. Seepage waters and gases were extracted and analysed over a period of three years (2004–2007) (Vinsot et al., 2008). Analytical data of water samples are shown in Table A-2. The analytical error for Na, Cl is 10% and for other solutes 5% (Vinsot, pers. communication).

HT experiment: This experiment also has an ascending borehole BHT-1 which was drilled with N_2 in 2010. Then the test interval was filled with Ar and the gas was circulated for one year (Vinsot et al., 2014). During this time, two seepage water samples were selected for chemical analyses (Table A-3). Then a hydrogen-neon-helium-argon mixture was injected which affected the compositions of the seepage waters, mainly by microbial reactions. The same analytical errors as for the PC-C experiment apply (Vinsot, pers. communication).

BN experiment: A descending vertical borehole BBN-1, which was drilled with N_2 in 2010, contains three separate test intervals, which were filled with N_2 (Bleyen et al., 2017). Subsequently, a solution similar to the expected porewater (denoted as artificial porewater) was continuously circulated through these intervals. Before injection of nitrate and other substances, the circulated water was sampled in the three test intervals. The analyses after eight months of diffusive equilibration with the surrounding porewater are shown in Table A-4. The analytical errors for major solutes vary in the range of 4–10% as indicated in Table A-4.

DR experiment: In this experiment, a descending borehole BDR-1 was drilled with N_2 in 2005. Artificial porewater was circulated through two separate test intervals until 2010 (Gimmi et al., 2014). Various tracers were injected to study their diffusion behaviour. The borehole waters which had equilibrated with the porewater for 4.5 years were analysed after termination of the experiment. Whereas the water from the upper interval was clearly affected by microbially disturbed conditions (Leupin et al., 2012), the analyses from the lower interval (Table A-5) were in line with the expected porewater composition. The analytical error is 10% for Na and Cl and 5% for the other solutes.

CI-4 experiment: In this experiment, artificial porewater was injected into a vertical descending borehole BCI-4 and diffusively equilibrated with the surrounding porewater for a period of 10 years (2006–2016) (Mäder, 2018). Samples were subsequently extracted via small PEEK capillaries and analysed for major and minor solutes. The two later samples, deemed to be less affected by disturbances compared to the first sample, are presented in Table A-6.

Early samples from seepage waters and groundwaters from the carbonate-rich lithologies of the bounding units (Passwang Fm. and Staffelegg Fm.) were analysed as reported by Pearson et al. (2003). Samples from a water-conducting zone in the Passwang Fm. were collected later by Waber and Rufer (2017). Data for Cl and other major solutes of these samples are presented in Table A-7.

3.3. Squeezed waters

The method of high-pressure squeezing of drillcores for obtaining porewater samples has been applied since the early days of the Mont Terri URL (Pearson et al., 2003). It has been successively improved, for example regarding measures to reduce sample oxidation during the squeezing process. Stepwise squeezing suggests that there is a formation-specific threshold pressure above which disturbing effects, such as shift in electrostatic equilibrium during the squeezing process, ion filtration and pressure solution of carbonates, affect solute chemistry (Fernández et al., 2014; Mazurek et al., 2015). In the following, the experiments where squeezed samples were obtained are summarised. All data are listed in Appendix B. The methodological approach and the analytical methods are detailed in Mazurek et al. (2015).

DB-A experiment: In this experiment, a borehole (BDB-1) was drilled inclined about perpendicular to bedding through limestones of the Hauptrogenstein Fm., the mixed calcareous-argillaceous lithologies of the Passwang Fm., the Opalinus Clay and the uppermost part of the underlying clay-rich Staffelegg Fm. A number of drillcores from the OPA and one from the Passwang Fm. were sampled for high-pressure squeezing (Mazurek et al., 2017). Squeezing was carried out at pressures of 125–500 MPa. Only data of the lowest squeezing pressure, deemed to be the least affected by disturbances mentioned above, were

Table 1
Borehole waters: Average compositions in mmol/L of all sample compositions in Tables A-1 to A-6 and errors in % (standard deviations of individual samples for PC-C, WS-A1, WS-A2, WS-A3 and range of individual samples for HT, BN and CI-4). For DR-II (lower interval) analytical error is given.

	PC-C	% error	WSA-1	% error	WSA-2	% error	WSA-3	% error	HT	% error	BN	% error	CI-4	% error	DR-II	% error
no. samples	9		20		7		16		2		3		2		1	
Dist. top OPA	122.4 m		101.9 m		67.9 m		36.1 m		100.5 m		66.5 m		93.4 m		51.8 m	
pH	7.13	*3.3*	7.56	*5.0*	7.34	*4.3*	7.38	*1.9*	7.25	*2.1*	7.23	*2.1*	7.13	*0.4*	7.54	*1.3*
Na	280.67	*2.0*	228.80	*5.5*	173.57	*6.7*	121.06	*5.3*	252.00	*7.9*	174.00	*0.0*	239.56	*1.9*	147.02	*10*
K	1.92	*37.8*	1.45	*13.1*	1.01	*15.9*	0.90	*23.3*	1.84	*32.6*	1.20	*0.0*	1.42	*2.7*	0.97	*5*
Mg	21.97	*2.2*	16.33	*3.6*	9.42	*27.2*	5.88	*3.7*	19.20	*5.2*	9.43	*3.2*	16.13	*2.0*	9.63	*5*
Ca	18.90	*2.9*	15.56	*4.1*	9.62	*13.8*	6.77	*6.1*	16.40	*1.2*	11.13	*4.5*	15.16	*2.0*	8.11	*5*
Sr	0.46	*13.6*	0.46	*4.7*	0.45	*9.2*	0.35	*6.6*	0.51	*17.6*	0.40	*0.0*	0.48	*4.8*	0.46	*5*
Cl	326.67	*1.7*	272.60	*6.4*	182.00	*5.0*	120.94	*7.0*	286.50	*4.5*	204.03	*0.7*	271.46	*2.8*	174.03	*10*
Br	0.34	*44.4*	0.45	*3.2*	0.29	*9.9*	0.20	*5.5*	0.45	*5.5*			0.50	*11.3*	0.98[a]	*5*
SO_4	16.79	*5.2*	12.59	*15.6*	11.75	*34.3*	7.44	*25.2*	16.30	*8.6*	11.45	*2.8*	13.54	*8.1*	8.58	*5*
Alkalinity	3.85	*19.7*	1.28	*83.0*	5.50	*36.4*	7.82	*88.7*	2.21	*10.9*			2.32	*0.6*	3.98	*5*
TIC	3.89	*14.4*	1.35	*29.4*	3.04	*51.6*	3.93	*14.4*	2.40	*1.7*	3.60	*33.3*	2.47	*4.0*	1.60	*5*
Fe	3.0E-02	*40.1*	3.5E-03	*91.4*	7.2E-03	*55.6*	4.5E-03	*0.0*	4.9E-02	*119.8*						
Si	0.17	*29.8*	5.4E-02	*42.3*	0.136	*29.7*	0.10	*27.8*	0.397	*102.1*			0.123	*8.7*		
Ba	6.1E-04	*34.2*	1.8E-04	*37.9*	7.9E-05		1.5E-04	*13.0*					<7E-4			
TOC (mg/L)	11.34	*39.1*	12.95	*60.9*	5.10	*60.3*	2.49	*88.5*	18.42	*115.3*	9.68	*13.6*	9.10	*18.1*	1.60	*10*

[a] Br used as tracer in experiment.

considered here (125–300 MPa; Table B-1). Analytical errors are 5% for major solutes and 10% for other solutes. The propagated relative uncertainty for the thus derived porewater concentration is about 10–15% (Waber and Rufer, 2017). It is worth noting that the BDB-1 borehole penetrated through OPA beds about 100–200 m below the level of the laboratory, where the thickness of the OPA is 130.6 m (Hostettler et al., 2017), slightly lower than along the laboratory tunnel (Pearson et al., 2003). To compare the spatial profiles of DB-A data with the other data from or nearby the laboratory level, the positions of the former data were scaled according to the procedure detailed in Wersin et al. (2020).

DR experiment: A drillcore of 2 m length was sampled from a borehole BDR-2 adjacent to BDR-1 used for borehole water sampling (see above) (Fernández et al., 2014). A squeezing pressure of 175 MPa was applied, yielding a water sample (Table B-2). The analytical error was 5% for all solutes except for Fe and K which were 10–20%.

HT experiment: A drillcore of 1 m length was sampled from the same borehole BHT-1 in which borehole waters were sampled (Fernández et al., 2014). Squeezing pressures of 75–200 MPa were applied. The data squeezed at these pressures indicated no systematic differences, but the data squeezed at the lowest pressure of 75 MPa is selected here (Table B-2). The analytical error was 5% for all solutes except for Fe and K which were 10–20%.

3.4. Leached waters

Aqueous leaching tests delivers inventories of free components not affected by mineral-water reactions (e.g. Cl, Br). This enables the determination of in-situ anion concentrations if water content, density and the anion-accessible porosity are known. In this study selected leachate data were used to refine the chloride and bromide profiles. For re-calculation to porewater concentration, the corresponding water contents and an anion-accessible porosity fraction (f_{an}) of 0.54 (Pearson et al., 2003) were considered. The relative error for re-calculated porewater concentrations was assumed to be 15%.

Chloride and bromide data from aqueous leaching tests on core samples of the BDB-1 borehole (Waber and Rufer, 2017) as well as older leachate data generated by different laboratories and synthesised by Pearson et al. (2003) were used to complement Cl and Br profiles. The experimental and analytical method of the leaching tests are presented in Pearson et al. (2003).

3.5. Cation exchange data

The cation exchange capacity (CEC) and the exchangeable cation occupancies are important parameters for modelling of porewaters in clayrocks (Gaucher et al., 2009; Pearson et al., 2011). The latter can be considered as "image" of major porewater cation composition (Tournassat et al., 2015). All data selected here is based on the Ni ethylene diamine (Ni-en) extraction method with a high solid/liquid ratio, which has been shown to yield coherent cation exchange parameters for OPA (Hadi et al., 2019). Moreover, the same correction for deriving cation occupancies was used in order to account for the contribution of solutes dissolved during extraction. This correction is based on the concentrations of the main anions Cl and SO_4 in aqueous extracts. Thus, Cl is subtracted from the extracted Na and SO_4 from the extracted Ca in the Ni-en extracts, respectively (Bradbury and Baeyens 1998). The other extracted cations Mg, K, Sr are not corrected for the derivation of cation occupancies. The methodology of determining and the exchangeable cation occupancies by Ni-en extraction is described in Waber et al. (2020).

With these premises in mind and the overall aim of selecting data representative of the entire formation, the following datasets were selected: data on early samples from drillcores of WS-E2, WS-E3, WS-A5 and WS-A6 experiments, as presented in Pearson et al. (2003), WS-A1 (Bradbury and Baeyens 1998) and more recent samples from the PC experiment (Koroleva et al., 2011) and the CI-4 experiment (Hadi et al., 2019). The raw data are shown in Appendix C (Table C-1). The analytical uncertainty of cation concentrations in Ni-en extracts is roughly 10%.

4. Results and discussion

4.1. Major solute data

Table 1 shows the averaged analyses of major solutes together with the estimated error for the borehole waters. The presented errors are based on the standard deviation for the experiments PC-C, WS-A1, WS-A2 and WS-A3 (7–20 samples per experiment) or the range for the

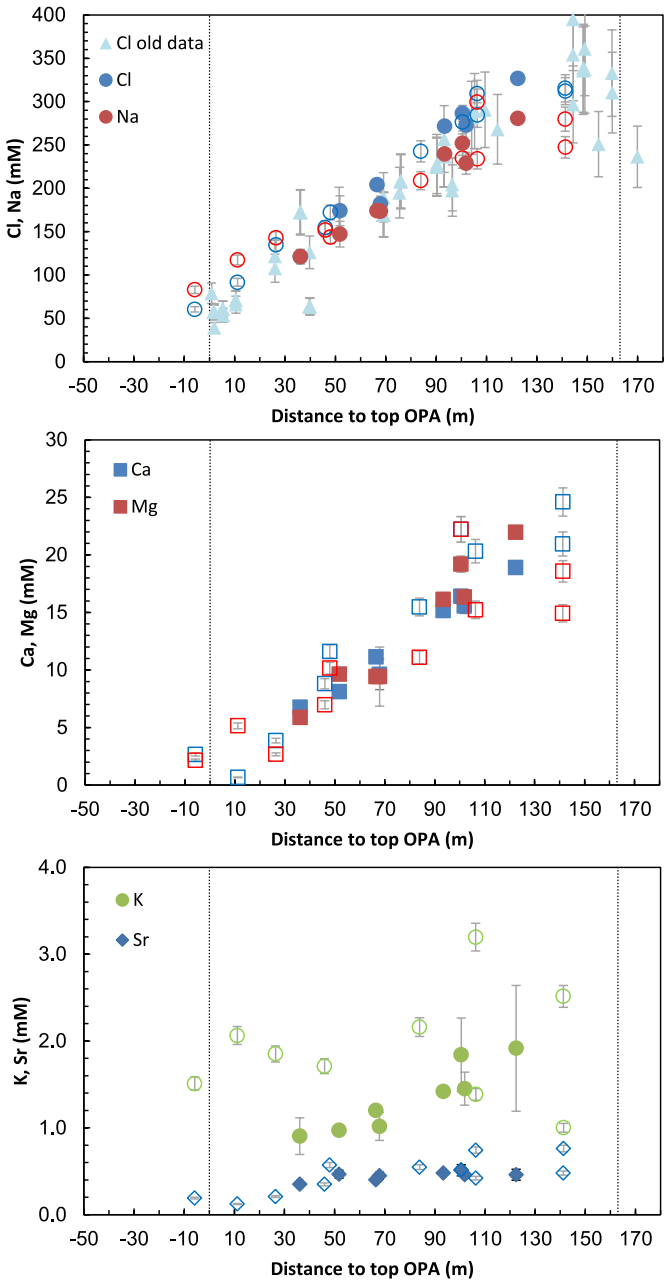

Fig. 4. Spatial profiles (orthogonal distance from top OPA) of Na, Cl (upper), Ca, Mg (central) and K, Sr (lower) in porewaters. Closed symbols: borehole waters; open symbols: squeezed waters, triangles (upper figure): "old" squeezed water and leachates from Pearson et al. (2003), dashed lines: boundaries of OPA. Squeezed waters: from borehole BDB-1 projected to laboratory level. All Cl data are also shown in Fig. 2.

experiments HT, BN and CI-4 (2–3 samples). For the DR experiment (1 sample), the analytical error is shown. The analyses of all individual samples are shown in Appendix A. Spatial profiles of major solutes, including also seepage and groundwater data from the Passwang Fm. and Staffelegg Fm., are presented in Appendix E (Fig. E−1).

The estimated errors of the concentrations of Cl and Na are within 7% and 8%, respectively, thus roughly in the same range as the analytical error of the individual samples (5–10%). The spatial profile of Na follows the same trend as Cl, thus exhibiting a steady increase with orthogonal distance from the top the OPA peaking at about 150 m (Fig. 4). The data of the squeezed waters (Table 2) are fully consistent with this trend (Fig. 4), but variations are slightly larger compared to borehole data. All waters are of Na–Cl type.

Ca and Mg concentrations of the borehole waters are in the same range and generally display small uncertainties, except for WSA-2 whose estimated error is well beyond the analytical error of the individual samples. Both cations exhibit a similarly increasing trend with distance from the OPA/Passwang Fm. contact (Fig. 4). The squeezed waters are consistent with this trend but display a somewhat larger scatter. K concentrations of borehole waters exhibit a steady increase from about 1 to 2 mM towards the lower beds of the OPA (Fig. 4). K concentrations in the squeezed waters show higher values and a larger scatter with no particular trend. Sr concentrations indicate an increasing trend for borehole and squeezed waters.

Estimated uncertainties of average sulphate concentrations in borehole waters are in the range of 3–34%, thus larger than for the other major solutes. An increase towards the footwall of the OPA starting at about 30 m from the top OPA is discerned (Fig. 5). The squeezed waters have a similar trend, but with more scatter. The uppermost three squeezed samples suggest a decreasing trend, but no borehole data is available in this section which could confirm or disconfirm this trend. The seepage waters and groundwater from the Passwang Fm. and Staffelegg Fm. display lower sulphate concentrations, as observed for Cl.

The overall profile does not appear to be strongly affected by oxidation phenomena. In fact, the SO_4/Cl ratio remains constant within the data error over most of the profile (Fig. 5). The same trend was noted for early data not affected by sulphide oxidation, as described by Pearson et al. (2003), who noted that the SO_4/Cl ratio is close to that of modern seawater (~0.052 mol/mol). This is also illustrated in Fig. 5 for most of the data. Towards the upper boundary of the OPA, however, SO_4/Cl ratios from squeezing data indicate an increase. According to Waber and Rufer (2017) this ratio further increases within the Passwang Fm. towards the aquifer, reaching a molar ratio of ~9 in the groundwater sample at about 50 m from the OPA/Passwang Fm. boundary (Fig. 5).

In summary, borehole waters and squeezed waters are broadly consistent, although the latter exhibits somewhat more scatter. For K, the squeezed waters point to higher concentrations, the reason of which is not known at this stage. The spatial profiles of all major solutes are similar to that of Cl, which was interpreted to be dominated by diffusive exchange with bounding aquifers (section 2.2). It is thus suggested that the profiles of all major solutes are also dominated by diffusive exchange, but coupled to cation-exchange reactions. In the case of sulphate, it should be noted, however, that there is some uncertainty regarding the significance of the squeezed data close to the OPA/Passwang Fm. boundary.

4.2. Cation exchange data

Table 3 shows the CEC values derived from the consumption of the index cation (Ni) as well as the corrected exchanger composition and cation occupancies. The profiles of the cation occupancies are depicted in Fig. 6 as bold squares. Na, Ca, and K reveal small variations between individual samples within the analytical errors. For Mg, sample variations are somewhat larger. The cation exchange data indicate a decrease in Na occupancies towards the top of the OPA. Mg, K and Sr suggest a slightly increasing trend, but for Ca no clear trend can be discerned.

Table 2
Squeezed waters: Compositions in mmol/L. Complete data including analytical errors shown in Table B-1 & B-2.

Sample ID	DB_100	DB_115	DB_127	DB_143	DB_174	DB_192	DB_193	DB_221	DB_222	HT-1m	DR-2m
Formation	PassW	OPA	OPA	OPA	OPA	OPA	OPA	OPA	OPA	OPA	OPA
Dist. top OPA	−5.82 m	11.15 m	26.41 m	45.96 m	83.89 m	106.26 m	106.32 m	141.25 m	141.31 m	100.5 m	48.0 m
pH	8.56	8.98	8.34	7.93	8.02	7.61		7.37		7.70	7.30
Na	82.86	117.23	142.92	151.80	208.85	243.90	234.01	279.71	247.38	234.89.42	143.54
K	1.51	2.06	1.85	1.71	2.16	2.05	1.38	2.51	1.00	1.41	0.51
Mg	2.16	5.14	2.67	6.97	11.10	12.15	15.22	14.92	18.58	22.22	10.16
Ca	2.65	0.67	3.86	8.80	15.47	17.90	20.32	20.95	24.60	16.79	11.60
Sr	0.19	0.12	0.21	0.35	0.55	0.48	0.74	0.48	0.76	0.51	0.57
Cl	60.28	91.53	134.73	154.75	242.61	276.69	284.50	315.39	312.16	276.42	172.06
Br	0.11	0.13	0.19	0.23	0.35	0.41	0.42	0.45	0.44	0.38	0.24
SO_4	12.61	9.97	8.03	12.97	12.04	15.15	16.03	17.26	16.69	17.70	13.53
Alkalinity				2.83	3.41		0.42			1.82	1.50
TIC		14.65		2.30	1.78						

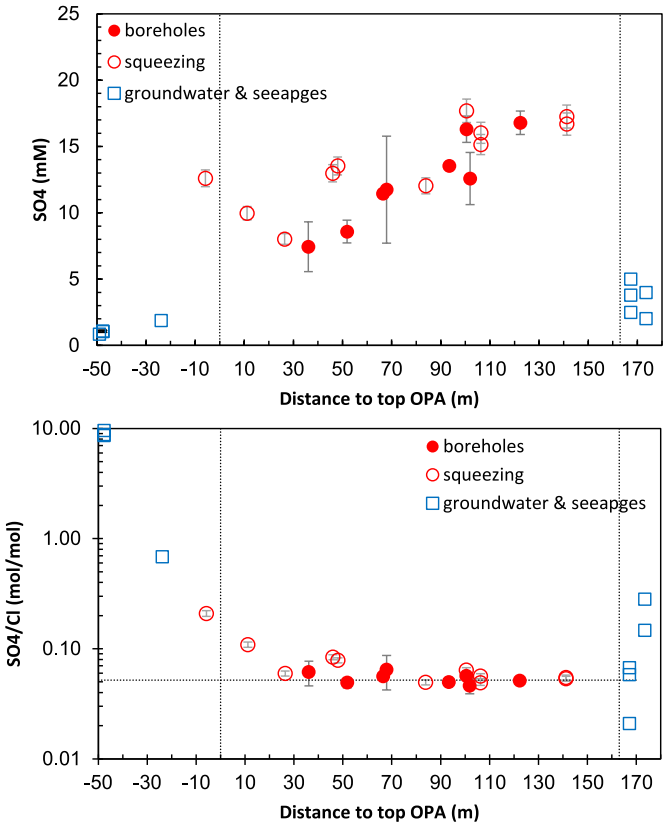

Fig. 5. Spatial profiles (orthogonal distance from top OPA) of SO_4 (upper) and SO_4/Cl molar ratio (lower) in porewaters. Dashed horizontal line: molar ratio of modern seawater, dashed vertical lines: boundaries of OPA. Squeezed waters: cores from BDB-1 projected to laboratory level. Groundwaters and seepages from Pearson et al. (2003) and Waber and Rufer (2017).

The adequacy of the cation exchange data can be tested by using the independent porewater dataset presented above. This was done by applying the well-established single-site Gaines-Thomas type cation exchange model developed for OPA and the Callovo-Oxfordian Fm (Gaucher et al., 2009; Pearson et al., 2011). as shown in Table C-2. The geochemical code PHREEQC V3 (Parkhurst and Appelo, 2013) and the thermodynamic database THERMOCHIMIE (Giffaut et al., 2014) was used for this purpose. Temperatures of 13 °C and 22 °C were assumed for the borehole waters and squeezed waters, respectively. Furthermore, a constant CEC value of 100 meq/kg, a grain density of 2.71 g/cm^3 and a porosity of 0.136 were considered in the calculations. The values are based on the compilation on core samples of the BDB-1 borehole (Mazurek and Aschwanden, 2020) who report median values of 2.706 (±0.0114) and 0.136 (±0.022) for the grain density and (water-loss) porosity, respectively. Note that the absolute value of the CEC is not a sensitive parameter for the derivation of cation occupancies.

The modelled cation occupancies for the borehole waters are also illustrated in Fig. 6 (circles). For Na, Ca and Mg and K the data are consistent with the measured (and corrected) occupancies. The modelled cation occupancies for the squeezed waters show slightly more scatter and, in the case of Na and Mg, slightly inferior agreement with the measured exchanger composition near the top OPA, but are broadly consistent with the measured data.

The agreement between the measured and modelled K occupancies of borehole waters using a high selectivity coefficient as proposed by Gaucher et al. (2009) and Pearson et al. (2011) is rather good (Fig. 6) and confirms the high affinity of K to the OPA. For Mg, both the modelled and the measured data show a considerable scatter. This particularly holds for the squeezed water data.

In summary, the major cations Na, Ca, Mg and K measured in the borehole and squeezed waters show a general consistency with the cation exchange data. Borehole waters appear to display a slightly better match than squeezed waters.

The measured Sr occupancies are systematically higher than the calculated ones, especially near the top OPA (Fig. 6). The higher measured Sr occupancy compared to the modelled one was also noted for the Callovo-Oxfordian clayrock in the eastern Paris Basin (COx) (Gaucher et al., 2009) who explained this by selective dissolution of $SrSO_4$ during the extraction. For the measurements and the data calculated from borehole waters, there is an increase of Sr occupancies from the lower part to the upper part of the OPA.

The Sr occupancy (together with the other cation occupancies) is used as input parameter in the geochemical modelling of porewater compositions in OPA (Mäder, 2009; Wersin et al., 2016) and COx (Gaucher et al., 2009). Because of side reactions, such as $SrSO_4$ dissolution occurring during extraction of exchangeable cations, the Sr occupancy is poorly constrained, resulting in uncertainties in predictions of porewater compositions. The Sr occupancies calculated from the borehole waters exhibit a linear decrease with increasing distance from the top OPA, therefore also a linear negative correlation with chloride concentrations (Fig. E−2). As expected from the near-to-constant SO_4/Cl ratio, the same type of correlation is seen between Sr occupancies and sulphate concentrations. This can be reasoned by the establishment of celestite equilibrium (see next section) during diffusive exchange of SO_4 with the bounding upper aquifer.

4.3. *pH/pCO_2 conditions and carbonate mineral equilibria*

The pH values of boreholes waters range from 7.1 to 7.6 (Table 1) and do not exhibit any dependency with distance across the formation. On the other hand, pH values of squeezed waters show a large scatter ranging from 7.3 to 9, with most values above those obtained from the borehole waters. Alkalinity and/or TIC data for squeezed waters are

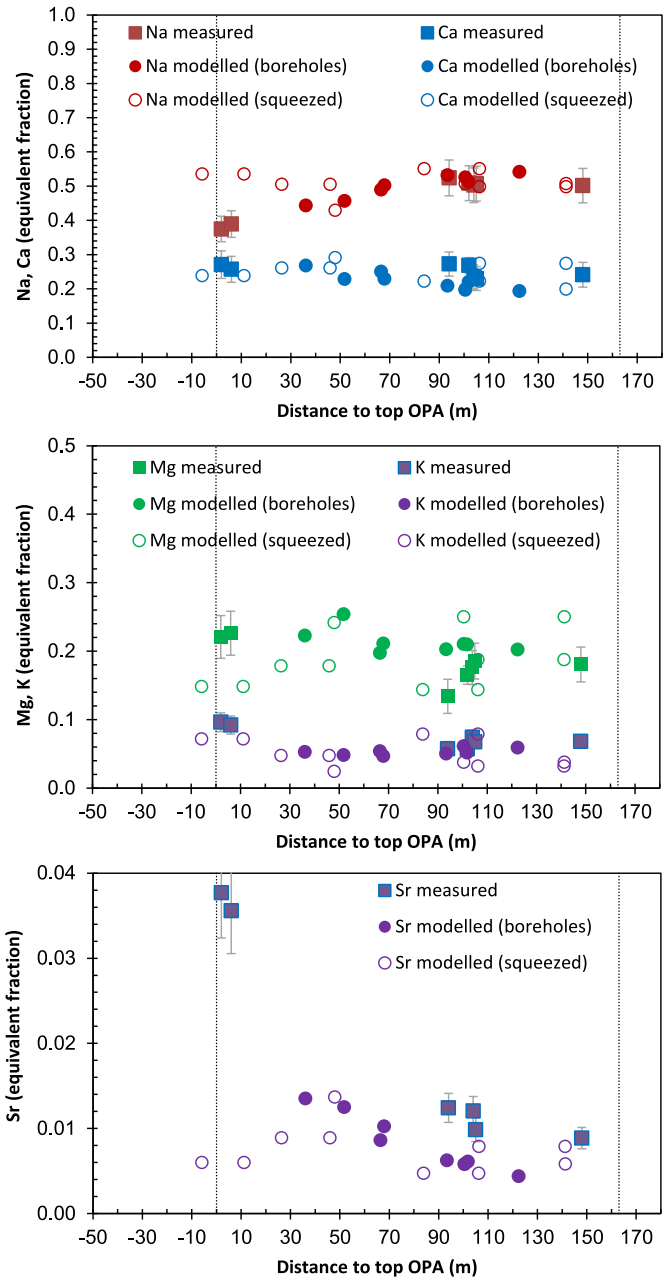

Fig. 6. Spatial profiles (orthogonal distance to top OPA) of exchangeable Na and Ca (upper), Mg and K (central) and Sr (lower) occupancies in OPA. Squares: measured data (Ni-en extraction); closed circles: modelled data from borehole waters, open circles: modelled data from squeezed waters (see text).

rather sparse (Tables B1 & B2). Using these data for speciation calculations reveals strong oversaturation with regard to calcite (except for sample DR). In contrast, for borehole waters, saturation indices for calcite are close to zero, which is expected in view of the widespread presence of this mineral. The pH conditions in the squeezed waters are thus likely perturbed which is explained by degassing of CO_2 during the squeezing process (Tournassat et al., 2015; Pearson et al., 2003). To address pH/pCO_2 conditions in the OPA, borehole water data thus appear more suitable.

Alkalinity data from borehole waters generally exhibit larger variations within the same experiment than TIC data. Therefore, calculation of pCO_2 and saturation indices for calcite and dolomite are based on the latter data. The CO_2 partial pressures derived from the pH and TIC values of the borehole waters are shown as function of distance from the OPA/Passwang Fm. contact in Fig. 7. They range between −2.9 and −2.0 log(bar), but the majority of the waters vary within −2.0 to −2.5 log(bar). Calculating pCO_2 by assuming calcite equilibrium rather than considering measured pH results in only minor differences (Fig. 7) because borehole waters are close to calcite equilibrium conditions. A priori, this is not an evidence that samples were not perturbed by CO_2(g) exchange, since a new equilibrium could have established in the sample via calcite precipitation in the case of CO_2 de-gassing and calcite dissolution in the case of CO_2 in-gassing. Furthermore it is noteworthy that perturbations of pH/pCO_2 conditions have little effect on major solutes due to the large cation exchange capacity of the clay. This is supported by the consistency in borehole, squeezing and cation exchange data as detailed above.

Measurement of CO_2(g) of degassing drillcores in sealed glass cells is another method to estimate pCO_2 as proxy for in-situ conditions (Pearson et al., 2003; Gaucher et al., 2010). Lassin et al. (2003), who

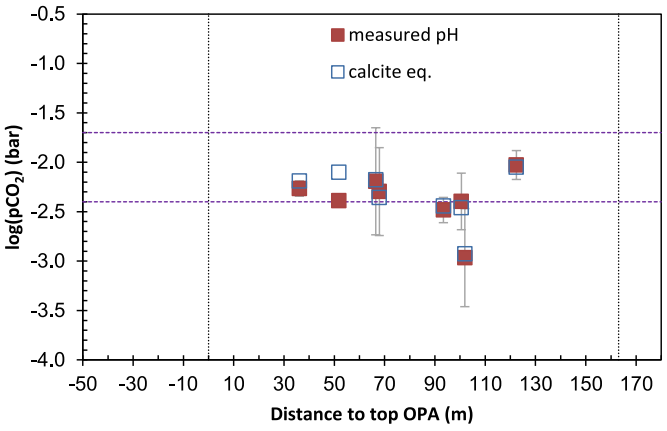

Fig. 7. Spatial profile (orthogonal distance from top OPA) of pCO_2 derived from borehole waters. Closed symbols: calculated from pH and TIC data; open symbols: calculated based on calcite equilibrium (adjusted pH values). Dashed lines: Lower and upper range of pCO_2 values derived by Vinsot et al. (2008) (see text).

Table 3
Average cation exchange capacity (derived from Ni consumption) and average exchangeable cation composition and cation occupancies corrected with NaCl/$CaSO_4$ procedure (see text). Original data shown in Table C-1. The error on raw data is presented in Table C-1. "eq. fr." = equivalent fraction.

Sample	Dist. top OPA	Ni cons.	Na	Ca	Mg	K	Sr	Na	Ca	Mg	K	Sr
			meq/kg					eq. fr.				
WS-A1 core	102 m	125.30	48.10	25.40	15.60	5.40		0.51	0.27	0.17	0.06	
PC core	104 m	109.00	54.20	25.30	19.00	8.00	1.30	0.50	0.23	0.18	0.07	0.012
CI core	94 m	133.00	54.80	28.50	14.00	6.00	1.30	0.52	0.27	0.13	0.06	0.012
WS-E2 core	2 m	91.70	36.09	26.05	21.25	9.25	3.63	0.37	0.27	0.22	0.10	0.038
WS-E3 core	6 m	93.80	37.86	25.00	22.00	5.40	3.46	0.39	0.26	0.23	0.09	0.036
WS-A5 core	105 m	115.10	51.55	23.36	18.85	6.85	1.00	0.51	0.23	0.19	0.07	0.010
WS-A6 core	148 m	115.50	66.25	31.85	23.85	9.00	1.17	0.50	0.24	0.18	0.07	0.009

Table 4
Calculated average pCO_2 and saturation indices (S.I.) of different minerals for borehole waters. Error represents standard deviation (PC–C, WS-A1, WSA-2, WSA-3) or range (HT, BN, CI-4) from individual samples.

Experiment	Dist. Top OPA	pCO_2 log (bar)	*error*	Calcite S.I.	*error*	Dolomite S.I.	*error*	Celestite S.I.	*error*	Barite S.I.	*error*	Gypsum S.I.	*error*	Quartz S.I.	*error*
PC-C	122.4 m	−2.03	*0.15*	−0.04	*0.11*	−0.01	*0.22*	−0.08	*0.07*	0.57	*0.14*	−0.45	0.02	0.11	*0.13*
WSA-1	101.9 m	−2.97	*0.50*	−0.03	*0.34*	−0.04	*0.66*	−0.13	*0.07*	−0.01	*0.15*	0.07	0.07	−0.42	*0.22*
WSA-2	67.9 m	−2.30	*0.44*	0.14	*0.41*	0.29	*0.80*	−0.05	*0.13*	−0.17		−0.71	0.12	0.02	*0.13*
WSA-3	36.1 m	−2.27	*0.08*	0.08	*0.16*	0.13	*0.32*	−0.20	*0.11*	0.05	*0.00*	−0.90	0.11	−0.10	*0.12*
HT	100.5 m	−2.40	*0.29*	−0.08	*0.31*	−0.07	*0.59*	0.00	*0.10*			−0.48	0.02	0.44	*0.49*
BN	66.5 m	−2.19	*0.54*	−0.03	*0.20*	−0.11	*0.40*	−0.10	*0.00*			−0.65	0.01		
CI-4	93.4 m	−2.48	*0.13*	0.05	*0.10*	0.13	*0.20*	−0.08	*0.02*			−0.56	0.02		
DR-II	51.8 m	−2.39		0.28		0.66		−0.10				−0.84			

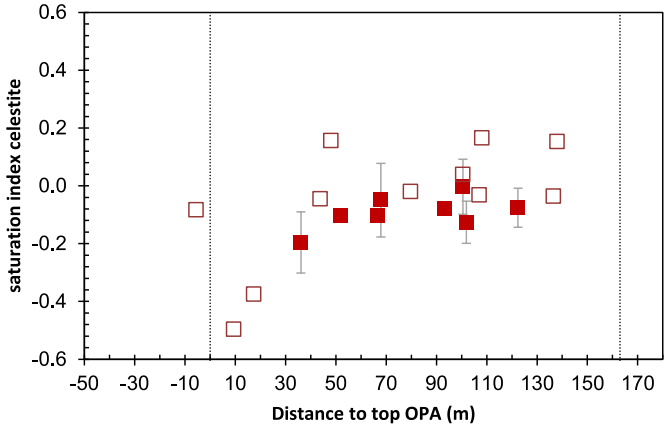

Fig. 8. Spatial profiles (orthogonal distance from top OPA) of saturation indices of celestite. Filled squares: borehole waters. Open squares: squeezed waters.

conducted pCO_2 measurements on two samples (A-6 and BG-2), derived a pCO_2 value of -2.2 ± 0.1 log(bar). Vinsot et al. (2008) derived pCO_2 values of −2.4 to −1.7 from a series of pH and alkalinity/TIC measurements in the PC-C experiment. This range as well as the pCO_2 measurements of Lassin et al. (2003) are consistent with the range inferred from the borehole data.

As observed for pH, the pCO_2 data does not indicate any dependency with distance from the contacts, thus no dependency on chloride concentrations. Such dependency was discussed by Pearson et al. (2003) based on early data. With the more recent data at hand, such a dependency can no longer be defended, the data rather suggest constant pCO_2 conditions. Internal control of the pCO_2 by silicate mineral equilibria would explain such constant pCO_2 across the formation at variable ionic strength and compositions (Gaucher et al., 2009). Assuming equilibrium with different pairs of clay minerals (kaolinite, illite, montmorillonite, and chlorite), Pearson et al. (2011) derived pH values of 7.3–7.8 and corresponding alkalinities of 1.3–0.3 mM based on equilibrium modelling of the PC-C experiment. This results in pCO_2 values of −2.5 to −3.5 log(bar), which is in a similar range, albeit slightly lower than derived from the porewater chemistry data. It should be noted that there is significant uncertainty in underlying thermodynamic data for clay minerals (Pearson et al., 2011) and, in a more general sense, the adequacy of assuming equilibrium with clay mineral phases, such as illite or montmorillonite, has been questioned (Lippmann 1982; Essene and Peacor 1995).

As mentioned above, borehole waters are close to saturation with regard to calcite when calculated from TIC values. Using alkalinity data instead results in more variations, suggesting more uncertainty in the latter data. The waters are generally not far from equilibrium with regard to dolomite, although variations in the individual samples (shown as errors of the averaged S.I. values in Table 4) are considerable and distinctly larger than those of the individual calcite S.I. values.

4.4. Constraints for sulphate

Sulphate shows the same trend as chloride over most of the profile, which is manifested by a constant SO_4/Cl ratio across most of the profile (Fig. 5). Towards the upper formation boundary, this ratio rises, as indicated from squeezing data. This trend continues in the Passwang Fm. up to the bounding aquifer located about 50 m from the upper OPA boundary (Griffault et al., 2003; Waber and Rufer, 2017). This behaviour suggests diffusive exchange between the porewater and the adjacent groundwater over the last few million years, as postulated for conservative solutes Cl and water tracers (Mazurek et al., 2011). The sulphate levels in this groundwater are low, thus lying within the generally decreasing trend within the OPA. The three uppermost squeezed waters from the BDB-1 borehole, however, fall off this trend, even suggesting an increase in this section. The significance of these samples is uncertain and, so far, no borehole data at laboratory level is available which could support these data. Conversely, the seepage waters in the underlying Staffelegg Fm. close to the lower OPA boundary display SO_4/Cl ratios which are more in line with those observed in the OPA porewater (Fig. 5). The scatter of these seepages, which were sampled in the 1990ies (Pearson et al., 2003), is large, suggesting perturbed conditions during sampling.

All waters are clearly undersaturated with regard to gypsum (Table 4). Sulphate concentrations are however in line with celestite equilibrium. Borehole waters exhibit a narrow range in S.I. values whereas squeezed waters show a larger spread (Fig. 8). Celestite containing various amounts of Ba has been observed in veins and as diagenetic mineral in OPA at Mont Terri (Lerouge et al., 2016; Pekala et al., 2018) and at other locations (Lerouge et al., 2014; Wersin et al., 2016). Celestite may occur as large elongated irregularly-shaped grains of several hundreds of μm, but also as smaller-sized grains in the range of 10–20 μm in the silty sub-unit and 2–4 μm in the shaly sub-unit (Jenni et al., 2019). Close to the upper boundary, the two squeezed water samples suggest undersaturation with regard to celestite. This might be explained by depletion of celestite in this boundary zone by some process in the past, but further data would be needed to confirm this hypothesis.

The presence of Ba in celestite (up to 20 wt% of Sr + Ba) raises the question whether porewater compositions are controlled by a (Ba,Sr)SO_4 solid solution or rather by equilibrium with pure celestite and barite. Applying different regular binary solid solution models to selected borehole waters, Pekala et al. (2018) concluded that a solid solution does not lead to a superior match of Sr and SO_4 borehole data, but to an inferior fit of the corresponding Ba data. Available data suggest in fact that borehole waters are in equilibrium with (pure) barite although there is scatter in the data (Table 4).

4.5. Redox conditions

Borehole waters exhibit reducing conditions as indicated from available Eh measurements. These, however, show large variations in the same borehole (Table A1). It should be noted that Eh measurements

Table 5
Eh_{SHE} values, Fe and Mn concentrations and saturation indices (S.I.) of siderite for borehole waters. Average values from individual samples for Eh (Tables A-1), errors from standard deviation (PC–C, WSA-1, WS-A2, WS-A3) and from range (HT).

Experiment	Dist. top OPA	Eh	*error*	Fe	*error*	Mn	*error*	Siderite	*error*
	m	mV		mM		mM		S.I.	
PC-C	122.4 m	<200[a]		2.96E-02	*1.19E-02*	6.88E-03	*1.51E-03*	−0.64	*0.21*
WS-A1	101.9 m	−96.15	*156*	3.5E-03	*3.2E-03*	6.3E-03	*5.1E-03*	−1.42	*0.53*
WS-A2	67.9 m	−5.57	*203*	7.2E-03	*4.0E-03*	3.6E-03	*7.6E-04*	−0.93	*0.18*
WS-A3	36.1 m	−18.71	*115*	4.4E-03	*5.0E-03*	5.5E-03	*1.7E-03*	−0.95	*0.72*
HT	100.5 m			4.91E-02	*4.16E-02*			−0.89	*−0.02*

[a] Detailed data not reported by Vinsot et al. (2008).

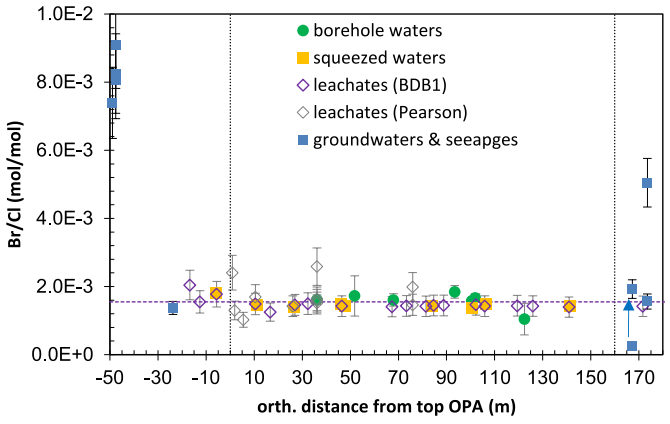

Fig. 9. Spatial profiles (orthogonal distance from top OPA) molar Br/Cl ratio. Dashed horizontal line: molar seawater ratio. Leachates back-calculated considering water-loss porosity and average anion-accessible porosity fraction of 0.54. Errors: 5% for squeezed waters, 10% for borehole waters, "old" squeezed waters and groundwaters/seepage waters, 15% for leachates. Arrow shows temporal evolution of a seepage water and groundwater in the Staffelegg Fm. (Gautschi et al., 1993).

in general are prone to sampling and analytical artefacts and also from theoretical considerations they should be interpreted with care (Pearson et al., 2003). The analyses of redox active elements Mn and Fe (Table A1-A3) confirm reducing conditions in the OPA porewater. Sulphide levels were generally found to be below detection limit, although at some instances sulphide was detected during sampling, such as for example in the PC-C experiment (Vinsot et al., 2008) and WSA-3 (Pearson et al., 2003) boreholes (Table A-1).

Control of the redox potential and Fe(II) by the pyrite/SO_4 couple and siderite equilibrium is commonly assumed for porewater chemistry modelling in OPA (Pearson et al., 2011), the COx formation (Gaucher et al., 2009) and the Boom Clay (De Craen et al., 2004; Mijnendonckx et al., 2019). Pearson et al. (2003) argued that, given the long residence times of the porewater solutes, the assumption sulphide/sulphate redox equilibrium was reasonable in spite of the probable absence of microbial activity in the nanoporous OPA. Control of redox potential by ferrous and ferric iron species was deemed to be less likely because of the lack of evidence of iron (oxyhydr)oxides. Moreover, measured Fe data were not consistent with the assumption of such control. It should be noted the dissolved total Fe data are sparse displaying large variations in the same borehole (Table A-1) and it is not clear to which extent they may have been affected by oxidation during sampling. The averaged Fe concentrations in fact suggest undersaturation with regard to siderite with S.I. values between −0.6 and −1.4 (Table 5), but uncertainties regarding the reliability of these data remain.

4.6. Other selected compounds

Silica: Dissolved Si concentrations in the borehole waters vary from about 4 to 50 μM (Table 1). Saturation indices for quartz scatter around zero (Table 4), which is consistent with the widespread occurrence of this mineral.

Dissolved organic carbon: Averaged concentrations of TOC vary roughly between 1 and 20 mg/L (Table 1). An increasing trend with distance from the OPA/Passwang Fm. contact, thus with increasing ionic strength is noted (Appendix E, Fig. E−3). According to the study of Courdouan Merz (2008) and Courdouan et al. (2007), about one third of the dissolved organic matter (DOM) in OPA consists of low molecular weight organic acids (acetate, lactate, formate, propionate) and one third of other unidentified hydrophylic compounds below a size of 500 Da. The remainder consists of hydrophobic (predominantly aliphatic) compounds. In general, the study revealed only small amounts of humic substances as also indicated from the study of Glaus et al. (2005). The DOM extracted with artificial anoxic porewater at high S/L ratio (Courdouan et al., 2007; Courdouan Merz 2008) displayed similar characteristics as that of seepage waters.

Bromide: This anion follows the same trend as chloride although data scatter is somewhat larger owing presumably to the larger analytical uncertainty of this minor anion (Fig. D-2). The same trend of the spatial profile is also manifested by a constant Br/Cl ratio across the entire OPA and part of the confining units (Fig. 9). The ratio corresponds to that of modern seawater (Appendix E, Fig. E−4), which is also the case for the SO_4/Cl ratio (Fig. 5) (see discussion above). This would suggest a marine origin of the porewaters. However, as discussed in Pearson et al. (2003) a marine origin is at odds with the stable water isotope signals. This apparent discrepancy was recently explained by Mazurek and De Haller (2017) with a rather complex paleo-hydrogeological model. Therein, current porewaters at Mont Terri were rationalised as mixtures between an old component in the Dogger units, a partially evaporated Tertiary seawater and more recent fresh groundwaters.

5. Conclusions

The analysis of borehole waters, squeezed waters and cation exchange experiments acquired over the last 25 years has enabled a unique porewater chemistry database of Opalinus Clay at the Mont Terri site. The results underline that the porewater composition is not constant but exhibits a regular change towards the formation boundaries. This is qualitatively – and at least for Cl also quantitatively – explained by diffusive exchange between the NaCl type porewater and the two bounding freshwater aquifers. Furthermore, the porewater is constrained by cation exchange, carbonate mineral and celestite equilibria. The following specific findings are worth mentioning:

- Major solute data (Cl, Na, SO_4, Ca, Mg, K) obtained from borehole waters and squeezed waters are broadly consistent. This supports the validity of squeezed waters as proxies for in-situ porewaters, although the data scatter is somewhat larger compared to borehole waters.
- pH, alkalinity and TIC data indicate effects of CO_2 gas exchange during drilling, sampling and/or experimental procedures, especially regarding squeezing data. Nevertheless, borehole data suggest that

the pCO_2 is constant across the formation, with a partial pressure in the range of −2.0 to −2.5 log(bar). This estimate is consistent with independent pCO_2 measurements on two drillcores. A constant pCO_2 of this order of magnitude can be explained by internal control via clay mineral equilibria.

- Reducing conditions prevail in the porewater owing to the presence of the reducing minerals, such as pyrite and siderite, and organic matter. Control of Eh by the pyrite/SO_4 redox couple has been assumed in the past, but control by the Fe(II)/Fe(III) redox couple cannot be ruled out at present. Fe concentrations suggest undersaturation with respect to siderite, but further data from well controlled experiments is required to reduce uncertainty in Fe concentrations and, more generally speaking, in understanding the controls of redox conditions.
- Overall, the knowledge on porewaters at the Mont Terri Rock Laboratory has significantly improved. In particular, this regards the spatial profiles of major elements besides Cl, and better constraints on exchanger composition and pH/pCO_2 conditions.

Declaration of competing interest

The authors declare that they have no known competing financial interests or personal relationships that could have appeared to influence the work reported in this paper.

Acknowledgements

This work has been made possible thanks to the Mont Terri Project and three decades of collaborations between the different involved institutions. We would like to mention fruitful discussions with Urs Mäder, Nick Waber, Lukas Aschwanden, Daniel Rufer, Andreas Jenni & Eric Gaucher (Uni Bern), Daniel Traber & Andreas Gautschi (Nagra), Marek Pekala (BASE), Agnès Vinsot (Andra), Christophe Tournassat (Uni Orléans), Joe Pearson (New Bern), Ana María Fernández (Ciemat), Tony Appelo (Amsterdam), David Jäggi & Christophe Nussbaum (swisstopo) and many other colleagues from the Mont Terri consortium. The comments of two anonymous reviewers have significantly helped to improve the manuscript. Funding from Nagra is acknowledged.

Appendix A. Supplementary data

Supplementary data to this article can be found online at https://doi.org/10.1016/j.apgeochem.2022.105234.

References

Altmann, S., 2008. 'Geo'chemical research: a key building block for nuclear waste disposal safety cases. J. Contam. Hydrol. 102, 174–179.

Appelo, C.A.J., Wersin, P., 2007. Multicomponent diffusion modeling in clay systems with application to the diffusion of tritium, iodide and sodium in Opalinus Clay. Environ. Sci. Technol. 41, 5002–5007.

Bleyen, N., Smets, S., Small, J., Moors, H., Leys, N., Albrecht, A., De Canniere, P., Schwyn, B., Wittebroodt, C., Valcke, E., 2017. Impact of the electron donor on in situ microbial nitrate reduction in Opalinus clay: results from the Mont Terri rock laboratory (Switzerland). Swiss J. Geosci. 110, 355–374.

Bossart, P., 2007. Overview of key experiments on repository characterization in the Mont Terri rock laboratory. 284, 35–40. Geol. Soc. London Spec. Publ. 284, 35–40.

Bossart, P., Wermeille, S., 2003. Paleohydrological study of the Mont Terri rock laboratory. In: Heitzmann, P., Tripet, J.P. (Eds.), Mont Terri Project– Geology, Paleohydrogeology and Stress Field of the Mont Terri Region. Federal Office for Water and Geology Rep. 4, Bern, pp. 45–64. Switzerland. www.swisstopo.admin.ch.

Bossart, P., Thury, M. (Eds.), 2008. Mont Terri Rock Laboratory Project, Programme 1996 to 2007 and Results. Reports of the Swiss Geological Survey No., vol. 3. Wabern, Switzerland.

Bradbury, M.H., Baeyens, B., 1998. A physicochemical characterisation and geochemical modelling approach for determining porewater chemistries in argillaceous rocks. Geochim. Cosmochim. Acta 62, 783–795.

Courdouan, A., Christl, I., Meylan, S., Wersin, P., Kretzschmar, R., 2007. Characterization of dissolved organic matter in anoxic rock extracts and in situ pore water of the Opalinus Clay. Appl. Geochem. 22, 2926–2939.

De Craen, M., Wang, L., Van Geet, M., Moors, H., 2004. The Geochemistry of Boom Clay Pore Water at the Mol Site, Status 2004. SCK•CEN Scientific Report. BLG 990.

Courdouan Merz, A., 2008. Nature and Reacivity of Dissolved Organic Matter in Clay Formations Evaluated for the Storage of Radioactive Waste. PhD Thesis. ETH Zurich.

Essene, E.J., Peacor, D.R., 1995. Clay thermometry - a critical perspective. Clay Clay Miner. 43, 540–553.

Fernández, A.M., Turrero, M.J., Sanchez, D.M., Yllera, A., Melon, A.M., Sanchez, M., Pena, J., Garralon, A., Rivas, P., Bossart, P., Hernán, P., 2007. On site measurements of the redox and carbonate system parameters in the low-permeability Opalinus Clay formation at the Mont Terri rock laboratory. Phys. Chem. Earth, Parts A/B/C 32, 181–195.

Fernández, A.M., Sánchez-Ledesma, D.M., Tournassat, C., Melón, A., Gaucher, E.C., Astudillo, J., Vinsot, A., 2014. Applying the squeezing technique to highly consolidated clayrocks for pore water characterisation: lessons learned from experiments at the Mont Terri Rock Laboratory. Appl. Geochem. 49, 2–21.

Freivogel, M., Huggenberger, P., 2003. Modellierung bilanzierter Profile im Gebiet Mont Terri – La Croix (Kanton Jura). In: Heitzmann, P., Tripet, J.P. (Eds.), Mont Terri Project – Geology, Paleohydrogeology and Stress Field of the Mont Terri Region, Federal Office for Water and Geology Rep., vol. 4. Bern, Switzerland, pp. 7–44. www.swisstopo.admin.ch.

Gaucher, E.C., Tournassat, C., Pearson, F.J., Blanc, P., Crouzet, C., Lerouge, C., Altmann, S., 2009. A robust model for pore-water chemistry of clayrock. Geochim. Cosmochim. Acta 73, 6470–6487.

Gaucher, E.C., Lassin, A., Lerouge, C., Fléhoc, C., Marty, N.C., Henry, B., Tournassat, C., Altmann, S., Vinsot, A., Buschaert, S., et al., 2010. CO_2 partial pressure in clayrocks: a general model. In: Water-Rock Interaction XIII - Water-Rock Interaction WRI-13. Mexico [hal-00664967 - version 1].

Gautschi, A., Ross, C., Scholtis, A., 1993. Pore water - groundwater relationships in jurassic shales and limestones of Northern Switzerland (ch. 17). In: Manning, D.A.C., H P, L., Hughes, C.R. (Eds.), Geochemistry of Clay - Pore Fluid Interactions. Chapman & Hall, London, pp. 412–422.

Giffaut, E., Grivé, M., Blanc, P., Vieillard, P., Colàs, E., Gailhanou, H., Gaboreau, S., Marty, N., Madé, B., Duro, L., 2014. Andra thermodynamic database for performance assessment: Thermochimie. Appl. Geochem. 49, 225–236.

Gimmi, T., Leupin, O., Eikenberg, J., Glaus, M.A., Van Loon, L.R., Waber, H.R., Wersin, P., Wang, H.A.O., Grolimund, D., Borca, C.N., Dewonck, S., Wittebroodt, C., 2014. Anisotropic diffusion at the field scale – I: a four-year multi-tracer diffusion and retention experiment at the Mont Terri Url (Switzerland). Geochim. Cosmochim. Acta 125, 373–393.

Glaus, M.A., Baeyens, B., Lauber, M., Rabung, T., Van Loon, L.R., 2005. Influence of water-extractable organic matter from Opalinus Clay on the sorption and speciation of Ni(II), Eu(III) and Th(IV). Appl. Geochem. 20, 443–451.

Griffault, L., Bauer, C., Waber, H.N., Pearson, F.J., Fierz, T., Scholtis, A., Degueldre, C., Eichinger, L., 2003. Water sampling and analyses for boreholes and seepages. In: Pearson, et al. (Eds.), Annex 1. Federal Office for Water and Geology, Bern, 2003.

Hadi, J., Wersin, P., Mazurek, M., Waber, H.N., Marques Fernandes, M., Baeyens, B., Honty, M., De Craen, M., Frederickx, L., Dohrmann, R., Fernandez, A.M., 2019. Intercomparison of CEC Method within the GD Project. Mont Terri Technical Report TR 2017-06.

Hostettler, B., Reisdorf, A.G., Jaeggi, D., Deplazes, G., Bläsi, H.R., Morard, A., Feist-Burkhardt, S., Waltschew, A., Dietze, V., Menkveld-Gfeller, U., 2017. Litho- and biostratigraphy of the Opalinus Clay and bounding formations in the Mont Terri rock laboratory (Switzerland). Swiss J. Geosci. 110, 22–39.

Jenni, A., Lanari, P., Aschwanden, L., de Haller, A., Wersin, P., 2019. Spectroscopic investigation of sulphate-controlling phases in OPA. Nagra Arbeitsbericht NAB 19–23. Wettingen, Switzerland.

Koroleva, M., Lerouge, C., Mäder, U., Claret, F., Gaucher, E., 2011. Biogeochemical processes in a clay formation in situ experiment: Part B – results from overcoring and evidence of strong buffering by the rock formation. Appl. Geochem. 26, 954–966.

Lassin, A., Gaucher, E.C., Crouzet, C., 2003. Dissolved carbon dioxide and hydrocarbon extraction. In: Pearson, F.J., et al. (Eds.), Geochemistry of Water in the Opalinus Clay Formation at the Mont Terri Rock Laboratory. Geology Series. No.5. Swiss Federal Office for Water and Geology. Annex 6, (Bern).

Lerouge, C., Grangeon, S., Claret, F., Gaucher, E.C., Blanc, P., Guerrot, C., Flehoc, C., Wille, G., Mazurek, M., 2014. Mineralogical and isotopic record of diagenesis from the Opalinus Clay formation at Benken, Switzerland: implications for the modeling of pore-water chemistry in a clay formation. Clay Clay Miner. 62, 286–312.

Lerouge, C., Maubec, N., Wille, G., Flehoc, C., 2016. GD Experiment: Geochemical Data Experiment. Analysis of Carbonate Fraction in Opalinus Clay. Mont Terri Technical Note. TN 2014-92.

Leupin, O.X., Wersin, P., Gimmi, T., Mettler, S., Rösli, U., Meier, O., Nussbaum, N.C., Van Loon, L., Soler, J., Eikenberg, J., Fierz, T., van Dorp, F., Bossart, P., Pearson, F.J., Waber, H.N., Dewonck, S., Frutschi, M., Chaudagne, G., Kiczka, M., 2012. DR (Diffusion & Retention) Experiment: Synthesis Field Activities, Data and Modelling. Mont Terri Technical Report TR 2011-01.

Lippmann, F., 1982. The thermodynamic status of clay minerals. In: Developments in Sedimentology 25; 7th Internat. Clay Conference. Elsevier, pp. 475–485, 1982.

Mäder, U.K., 2009. Reference Pore Water for the Opalinus Clay and "Brown Dogger" for the Provisional Safety-Analysis in the Framework of the Sectorial Plan - Interim Results (SGT-ZE). Nagra Arbeitsbericht NAB, 09-14, Wettingen, Switzerland.

Mäder, U.K., 2018. CI Experiment: Sampling and Analysis of Opalinus Clay Pore Water from Test Interval BCI-4 (2015/2016). Mont Terri Technical Note TN 2015-128.

Mazurek, M., 2017. Gesteinsparameter-Datenbank Nordschweiz – Version 2. In: Nagra Arbeitsbericht NAB, vols. 17–56. Wettingen, Switzerland.

Mazurek, M., Aschwanden, L., 2020. Multi-site petrographic and structural characterisation of the Opalinus Clay. Nagra Arbeitsbericht NAB 19-44, Wettingen, Switzerland.

Mazurek, M., De Haller, A., 2017. Pore-water evolution and solute-transport mechanisms in Opalinus clay at Mont Terri and Mont russelin (Canton Jura, Switzerland). Swiss J. Geosci. 110, 129–149.
Mazurek, M., Alt-Epping, P., Bath, A., Gimmi, T., Waber, H.N., 2009. Natural Tracer Profiles across Argillaceous Formations: the CLAYTRAC Project. Nuclear Energy Agency, OECD, Paris, p. 361.
Mazurek, M., Alt-Epping, P., Bath, A., Gimmi, T., Waber, N., Buschaert, S., De Cannière, P., De Craen, M., Gautschi, A., Savoye, S., Vinsot, A., Wemaere, I., Wouters, L., 2011. Natural tracer profiles across argillaceous formations. Appl. Geochem. 26, 1035–1064.
Mazurek, M., Al, T., Celejewski, M., Clark, I.D., Fernandez, A.M., Jaeggi, D., Kennell-Morrison, L., Matray, J.M., Murseli, S., Oyama, T., Qiu, S., Rufer, D., St-Jean, G., Waber, H.N., Yu, C., 2017. Mont Terri DB-A experiment: comparison of pore-water investigations conducted by several research groups on core materials from the BDB-1 borehole. Mont Terri Project. Technical Report TR 2017-01.
Mazurek, M., Oyama, T., Wersin, P., Alt-Epping, P., 2015. Pore-water squeezing from indurated shales. Chem. Geol. 400, 106–121.
Mijnendonckx, K., Honty, M., Wang, L., Jacops, E., Provoost, A., Mysara, M., Wouters, K., De Craen, M., Leys, N., 2019. An active microbial community in Boom Clay pore water collected from piezometers impedes validating predictive modelling of ongoing geochemical processes. Appl. Geochem. 106, 149–160.
Nagra, 2002. Project Opalinus Clay: Safety Report. Demonstration of Disposal Feasibility for Spent Fuel, Vitrified High-Level Waste and Long-Lived Intermediate-Level Waste (Entsorgungsnachweis). Nagra Technical Report NTB 02-05. Wettingen, Switzerland.
Parkhurst, D.L., Appelo, C.A.J., 2013. Description of Input and Examples for PHREEQC Version 3: A Computer Program for Speciation, Batch-Reaction, One-Dimensional Transport, and Inverse Geochemical Calculations. No. 6-A43. US Geological Survey.
Pearson, F.J., 1999. What is the porosity of a mudrock? In: Aplin, A.C., Fleet, A.J., Macquaker, J.H.S. (Eds.), Muds and Mudstones: Physical and Fluid Flow Properties, vol. 158. Geological Society, London, Special Publications, pp. 9–21.
Pearson, F.J., Arcos, D., Bath, A., Boisson, J.Y., Fernández, A.M., Gäbler, H.-E., Gaucher, E., Gautschi, A., Griffault, L., Hernán, P., Waber, H.N., 2003. Geochemistry of Water in the Opalinus Clay Formation at the Mont Terri Rock Laboratory. Federal Office for Water and Geology, Bern. Series No. 5.
Pearson, F.J., Tournassat, C., Gaucher, E.C., 2011. Biogeochemical processes in a clay formation in situ experiment: Part E – equilibrium controls on chemistry of pore water from the Opalinus Clay, Mont Terri Underground Research Laboratory. Appl. Geochem. 26, 990–1008. Switzerland.
Pekala, M., Wersin, P., Rufer, D., 2018. GD Experiment: Geochemical Data Experiment. Mineralogy of Carbonate and Sulphate Minerals in the Opalinus Clay and Adjacent Formations. Mont Terri Technical Report TR 2018-03.
Reisdorf, A.G., Hostettler, B., Waltschew, A., Jaeggi, D., Menkveld-Gfeller, U., 2014. SO (Sedimentology of the Opalinus-Ton): Biostratigraphy of the Basal Part of the Opalinus-Ton at the Mont Terri Rock Laboratory. Mont Terri Project, Switzerland. Technical Report TR 2014-07.
Rufer, D., Waber, H.N., Gimmi, T., 2018. Identifying temporally and spatially changing boundary conditions at an aquifer–aquitard interface using helium in porewater. Appl. Geochem. 96, 62–77.
Sacchi, E., Michelot, J.-L., Pitsch, H., 2000. Porewater Extraction from Argillaceous Rocks for Geochemical Characterisation. Nuclear Energy Agency, OECD, Paris.
Thury, M., Bossart, P., 1999. Mont Terri Rock Laboratory. Results of Hydrogeological, Geochemical and Geotechnical Experiments Performed in 1996 and 1997. Swiss National Hydrological and Geological Survey, Bern, Switzerland.
Tournassat, C., Steefel, C.I., 2015. Ionic transport in nano-porous clays with consideration of electrostatic effects. Rev. Mineral. Geochem. 80, 287–329.
Tournassat, C., Vinsot, A., Gaucher, E.C., Altmann, S., 2015. Chemical conditions in clay-rocks. In: Tournassat, C., et al. (Eds.), Natural and Engineered Clay Barriers, Developments in Clay Science, vol. 6. Elsevier, pp. 71–100 (Chapter 3).
Vinsot, A., Appelo, C.A.J., Cailteau, C., Wechner, S., Pironon, J., De Donato, P., De Cannière, P., Mettler, S., Wersin, P., Gäbler, H.-E., 2008. CO_2 data on gas and porewater sampled in situ in the Opalinus clay at the Mont Terri rock laobratory. Phys. Chem. Earth 33, S54–S60.
Vinsot, A., Appelo, C.A.J., Lundy, M., Wechner, S., Lettry, Y., Lerouge, C., Fernandez, A. M., Labat, M., Tournassat, C., De Cannière, P., Schwyn, B., McKelvie, J., Dewonck, S., Bossart, P., Delay, J., 2014. Situ Diffusion Test of Hydrogen Gas in the Opalinus Clay, vol. 400. Geological Society, London, Special Publications, pp. 563–578.
Waber, H.N., Rufer, D., 2017. Porewater Geochemistry, Method Comparison and Opalinus Clay-Passwang Formation Interface Study at the Mont Terri URL. Mont Terri Technical Report 2017-02.
Waber, H.N. (Ed.), 2020. SGT-E3 Deep Drilling Campaign (TBO): Experiment Procedures and Analytical Methods at RWI. University of Bern (version 1.0, April 2020). Nagra Arbeitsbericht NAB 20-13, Wettingen, Switzerland.
Wersin, P., Gaucher, E.C., Gimmi, T., Leupin, O., Mäder, U., Thoenen, T., Tournassat, C., 2009. Geochemistry of Pore Waters in Opalinus Clay at Mont Terri: Experimental Data and Modelling. Mont Terri Technical Report TR 2008-06.
Wersin, P., Leupin, X.O., Mettler, S., Gaucher, E., Mäder, U., Vinsot, A., De Cannière, P., Gäbler, H.E., Kunimaro, T., Kiho, K., 2011. Biogeochemical processes in a clay formation in-situ experiment: Part A - overview, experimental design and water data of an experiment in the Opalinus Clay at the Mont Terri underground research laboratory, Switzerland. Appl. Geochem. 26, 931–953.
Wersin, P., Mazurek, M., Mäder, U.K., Gimmi, T., Rufer, D., Lerouge, C., Traber, D., 2016. Constraining porewater chemistry in a 250 m thick argillaceous rock sequence. Chem. Geol. 434, 43–61.
Wersin, P., Pekala, M., Mazurek, M., Gimmi, T., Mäder, U.K., Jenni, A., Rufer, D., Aschwanden, L., 2020. Porewater Chemistry of Opalinus Clay: Methods, Modelling & Buffering Capacity. In: Nagra Technical Report. Wettingen, Switzerland. NTB 18-01.